SUPPORTING INFORMATION

Ultra-thin Magnetic Film with Giant Phonon-drag for Heat to Spin Current Conversion

*Payal Wadhwa[1], Andrea Bosin[1], and Alessio Filippetti,[1,2]**

1 Dipartimento di Fisica, Università di Cagliari. S.P. Monserrato Sestu Km.0,700. Monserrato (Ca) 09042-I, Italy
2 Consiglio Nazionale delle Ricerche, Istituto Officina dei Materiali, CNR-IOM, S.P. Monserrato Sestu Km.0,700. Monserrato (Ca) 09042-I, Italy

* Corresponding author: alessio.filippetti@dsf.unica.it

S.1 Band model of electric and thermoelectric transport

In the framework of a multiband, spin-dependent approach, total conductivity and Seebeck coefficient are calculated as:

$$\sigma_j = \sigma_j^{\uparrow} + \sigma_j^{\downarrow} = \sum_{n\uparrow} \sigma_{n,j}^{\uparrow} + \sum_{n\downarrow} \sigma_{n,j}^{\downarrow} \tag{S.1}$$

$$S_j = \frac{\sigma_j^{\uparrow} S^{\uparrow}}{\sigma_j} + \frac{\sigma_j^{\downarrow} S^{\downarrow}}{\sigma_j} = \sum_{n\uparrow} \frac{\sigma_{n,j}^{\uparrow} S_{n,j}^{\uparrow}}{\sigma_j} + \sum_{n\downarrow} \frac{\sigma_{n,j}^{\downarrow} S_{n,j}^{\downarrow}}{\sigma_j} \tag{S.2}$$

where n is a band index running over up-spin and down-spin manifolds, and j the cartesian index; the spin-dependent Seebeck coefficients are defined as:

$$S_j^{\uparrow\downarrow} = \sum_{n\uparrow,\downarrow} \frac{\sigma_{n,j}^{\uparrow\downarrow} S_{n,j}^{\uparrow\downarrow}}{\sigma_j^{\uparrow\downarrow}} \tag{S.3}$$

Spin-dependent conductivities can be calculated according to the Bloch-Boltzmann Theory in relaxation time approximation:

$$\sigma_{n,j}^{\uparrow\downarrow} = \left(\frac{\mathrm{e}^2}{\mathrm{V}}\right)\int d\mathbf{k}\, g(\mathbf{k})\tau_{n\mathbf{k}}\left(-\frac{\partial f}{\partial \varepsilon_{n\mathbf{k}}^{\uparrow\downarrow}}\right)\left(v_{n\mathbf{k},j}^{\uparrow\downarrow}\right)^2 \tag{S.4}$$

$$S_{n,j}^{\uparrow\downarrow} = -\left(\frac{\mathrm{e}}{\mathrm{V}\,\mathrm{T}\,\sigma_{n,j}^{\uparrow\downarrow}}\right)\int d\mathbf{k}\, g(\mathbf{k})\tau_{n\mathbf{k}}(\varepsilon_{n\mathbf{k}}^{\uparrow\downarrow} - \varepsilon_F)\left(-\frac{\partial f}{\partial \varepsilon_{n\mathbf{k}}^{\uparrow\downarrow}}\right)\left(v_{n\mathbf{k},j}^{\uparrow\downarrow}\right)^2 \tag{S.5}$$

where V is the sample volume, f the Fermi occupancy, $\varepsilon_{n\mathbf{k}}$ and $v_{n\mathbf{k},j}$ band energies and velocities, respectively, g the density of states, $\tau_{n\mathbf{k}}$ the electronic relaxation time; for the latter, we assume an energy-dependent formulation derived by numerical models which has been largely tested in previous works, and includes electron scattering with impurities, acoustic phonons, and polar optical phonons. Also, we assume the spin-flip scattering discardable over our length scale of interest. The numerical integration of Eq. S.4 and S.5 based on ab-initio band energies is extremely demanding for large size systems, thus we adopt a parabolic band approximation for the conduction states which is totally adequate for our charge carriers of interest. We model the conduction band dispersion as:

$$\varepsilon_n^{\uparrow\downarrow}(\mathbf{k}) = \varepsilon_{n,0}^{\uparrow\downarrow} + \frac{\mathrm{h}^2}{2}\left(\frac{k_x^2}{m_{n,x}^*} + \frac{k_y^2}{m_{n,y}^*} + \frac{k_z^2}{m_{n,z}^*}\right) \tag{S.6}$$

where effective masses and band bottom energies are extracted from the calculated band structure for the Ti t_{2g} bands. Coherently with these results, Eq. S.6 assumes only the band bottom energies as spin-dependent, not the effective masses. Using Eq. S.6, we can rewrite S.4 and S.5 in terms of carrier energy:

$$\sigma_{n,j}^{\uparrow\downarrow} = \frac{\mathrm{e}^2\,\mathrm{C}_{n,j}}{k_B T}\int_{\varepsilon_{n,0}^{\uparrow\downarrow}}^{\infty} d\varepsilon\,\tau(\varepsilon)\left(-\frac{\partial f}{\partial \varepsilon}\right)\left(\varepsilon - \varepsilon_{n,0}^{\uparrow\downarrow}\right)^{3/2} \tag{S.7}$$

$$S_{n,j}^{\uparrow\downarrow} = -\frac{\mathrm{e}\,\mathrm{C}_{n,j}}{\sigma_{n,j}^{\uparrow\downarrow}\,k_B T^2}\int_{\varepsilon_{n,0}^{\uparrow\downarrow}}^{\infty} d\varepsilon\,\tau(\varepsilon)\left(-\frac{\partial f}{\partial \varepsilon}\right)(\varepsilon - \mu)\left(\varepsilon - \varepsilon_{n,0}^{\uparrow\downarrow}\right)^{3/2} \tag{S.8}$$

where $\beta = 1/k_B T$; the corresponding band occupancy is:

$$p_n^{\uparrow\downarrow} = D_n \int_{\varepsilon_{n,0}^{\uparrow\downarrow}}^{\infty} d\varepsilon\, f(\varepsilon)\left(\varepsilon - \varepsilon_{n,0}^{\uparrow\downarrow}\right)^{1/2} \qquad \text{(S.9)}$$

The coefficients *C* and *D* are:

$$\mathrm{C}_{n,j} = \frac{\sqrt{2}}{\pi^2 \mathrm{h}^3} \frac{\sqrt{m_{n,x}^* m_{n,y}^* m_{n,z}^*}}{m_{n,j}^*}; \qquad D_n = \frac{\sqrt{2}V}{\pi^2 \mathrm{h}^3} \sqrt{m_{n,x}^* m_{n,y}^* m_{n,z}^*} \qquad \text{(S.10)}$$

where *V* is the supercell volume.

S.2 Phonon-drag theory

The phonon-drag general theory has been developed in the past a long series of articles.[1-6] Here we adapt the formulation to an effective mass modeling built out on the basis the ab-initio calculated band structure for the Ti *3d* t_{2g} conduction states hosting the 2DEG. For phonons we consider a longitudinal acoustic phonon branch in linear approximation. The electron-phonon interaction is treated according to the deformation potential approach described by Cantrell and Butcher.[3,4] Only intra-band electron-phonon scattering is considered. In the following we give a brief outline of main formulas; the detailed formulation is described in the supporting information of Refs.7,8. From the coupled Boltzmann equation for electrons and phonons, the phonon-drag in the *j* direction is:

$$S_j^{\uparrow\downarrow} = \left(\frac{\mathrm{e}}{\sigma_{\mathrm{j}}^{\uparrow\downarrow} \mathrm{V}\, \mathrm{k_B T}^2}\right) n^{\uparrow\downarrow}{}_{,\mathbf{k},\mathbf{k}',\mathbf{q}} \sum \mathrm{h}\omega_{\mathbf{q}} \left(\frac{\Gamma_{n,\mathbf{k},\mathbf{k}'}(\mathbf{q})}{R_{ph}(\mathbf{q}) + R_{ep}^{\uparrow\downarrow}(\mathbf{q})}\right) V_j(n\mathbf{k}, n\mathbf{k}', \mathbf{q}) \qquad (S.11)$$

where $\boldsymbol{q}$ and $\omega_{\boldsymbol{q}}$ are phonon wavevector and frequency, respectively; $\Gamma_{n,\mathbf{k},\mathbf{k}'}(\mathbf{q})$ and $R_{ep}(\mathbf{q})$ are electron-acoustic phonon scattering rates:

$$\Gamma_{n,\mathbf{k},\mathbf{k}'}(\mathbf{q}) = f_{\mathrm{n}\mathbf{k}}\left(1 - f_{\mathrm{n}\mathbf{k}'}\right) N_q A_n(\mathbf{q})\, \delta\left(\varepsilon_{n\mathbf{k}'} - \varepsilon_{n\mathbf{k}} - \mathrm{h}\omega_{\mathbf{q}}\right) \delta_{\mathbf{k}',\mathbf{k}+\mathbf{q}} \qquad (S.12)$$

$$R_{ep}^{\uparrow\downarrow}(\mathbf{q}) = -\left(\frac{2}{N_q' k_B T}\right) \sum_{n^{\uparrow\downarrow},\mathbf{k},\mathbf{k}'} \Gamma_{n,\mathbf{k},\mathbf{k}'}(\mathbf{q}) \qquad (S.13)$$

where f_{nk} and Nq are Fermi-Dirac and Phonon equilibrium distributions, respectively, $A(\boldsymbol{q})$ is the electron-acoustic phonon coupling amplitude, $N_q' = dN_q / dq$, and the two delta functions impose energy and momentum conservation for the absorption process (the associated emission is implicitly included in the velocity factor); $R_{ph}(\mathbf{q})$ is the total phonon scattering rate (including phonon-phonon, phonon-boundary, and phonon-impurity scattering); the velocity factor is:

$$V_j(n\mathbf{k}, n\mathbf{k}', \mathbf{q}) = v_{q,j}\left[\tau_{n\mathbf{k}} v_{n\mathbf{k},j} - \tau_{n\mathbf{k}'} v_{n\mathbf{k}',j}\right] \qquad (S.14)$$

where $v_{q,j}$ is the phonon velocity. Eq. S.11 states that phonon-drag essentially depends on the ratio between the electron-phonon scattering and the total phonon scattering, so that it is only relevant where electron-phonon coupling dominates over other phonon scattering processes. ratio at the denominator. We approximate the velocities as:

$$v_{q,j} = v_s \hat{q}_j \qquad v_{nk,j} = \frac{\hbar k_j}{m_{nj}^*} \qquad (S.15)$$

where v_s is the sound velocity; we use momentum conservation $\delta_{k,k'} = \delta_{k,k+q}$ and assume $\tau_{nk} = \tau_{nk'}$; also, we express band energies in parabolic band approximation (Equation S.6), changing integration variables from k to energy; after rather lengthy manipulations we obtain:

$$S_j^{\uparrow\downarrow} = -\left(\frac{V e v_s}{12\pi^4 \hbar^3 \sigma_j^{\uparrow\downarrow} k_B T^2}\right) \sum_{n^{\uparrow\downarrow}} \sqrt{\frac{m_{nx} m_{ny} m_{nz}}{m_{nj}}} \int_{\varepsilon_{n,0}^{\uparrow\downarrow}}^{\infty} d\varepsilon\, f(\varepsilon)\tau(\varepsilon)\left(1 - f\left(\varepsilon + \hbar\omega_q\right)\right)$$
$$\times \int dq\, q^2 \left(\frac{\hbar\omega_q N_q A_n(q)}{R_{ph}(q) + R_{ep}^{\uparrow\downarrow}(q)}\right) \qquad (S.16)$$

The electron-phonon coupling cross section based on the deformation potential approach for a 2DEG is :

$$A_n(q) = \frac{\pi D^2 q^2}{\rho V \omega_q} \left(\int_t dz\, \psi_n^2(z)\, e^{iq_z z} \right)^2 = \frac{\pi D^2 q^2}{\rho V \omega_q} F_n\left(q_z\right) \qquad (S.17)$$

where D is the deformation potential, ρ the mass density, $\psi(z)$ the wavefunction of the 2D localized electrons, t the 2DEG thickness. When t is much smaller than the acoustic phonon wavelength in the z directions ($t << 2\pi / q_z$) $F_n(q_z)$: 1. Proceeding in similar way we obtain:

$$R_{ep}^{\uparrow\downarrow}(q) = \left(\frac{2\sqrt{3} V N_q A_n(q)}{(2\pi)^2 \mathsf{h}^4 q N_q' K_B T} \right) \sum_{n^{\uparrow\downarrow}} m_n^{2D} \int_{\varepsilon_{n,0}^{\uparrow\downarrow}}^{\infty} d\varepsilon\, f(\varepsilon) \left(1 - f(\varepsilon + \mathsf{h}\omega_q)\right) \quad (S.18)$$

where:

$$m_n^{2D} = \frac{m_{nx} m_{ny} m_{nz}}{\sqrt{m_{nx} m_{ny} + m_{nx} m_{nz} + m_{ny} m_{nz}}} \qquad (S.19)$$

Finally, the phonon scattering rate is expressed according to the modeling of Callaway[9]

$$\tau_{\mathrm{ph}}^{-1}(q) = \mathrm{A}\omega_q^4 + BT^3 \omega_q^2 + \frac{v_s}{L} \qquad (S.20)$$

where A describes scattering by point impurities, B the phonon-phonon scattering including both normal (crystal momentum-conserving) and umpklapp scattering, and v_s / L the boundary scattering (L is a characteristic sample length). Here we have used the same values $A = 0.5 \times 10^{-41}$, $B = 0.5 \times 10^{-20}$ K^{-3}, and $L = 0.1$ mm used in Ref. 8 for the STO/LAO interface.

S.3 Model parameters

We use effective mass values of 0.52 m_e and 5.43 m_e for the longitudinal and transversal direction of the t_{2g} states. For electronic and static dielectric constants ε_∞ and ε_0 we use IR measured values[10] of 5.88 and 160, respectively. The LO phonon energies extrapolated from plasma frequency measurements are $\omega_{LO,1}$ = 19 meV, $\omega_{LO,2}$ = 60 meV, $\omega_{LO,3}$ = 92 meV. The

deformation potential calculated from our band structure is D = 3.74 eV, and for the sound velocity we use the STO value $v_s = 1.5\times10^5$ cm/s.

S.4 Results for 2-ETO layer heterostructure

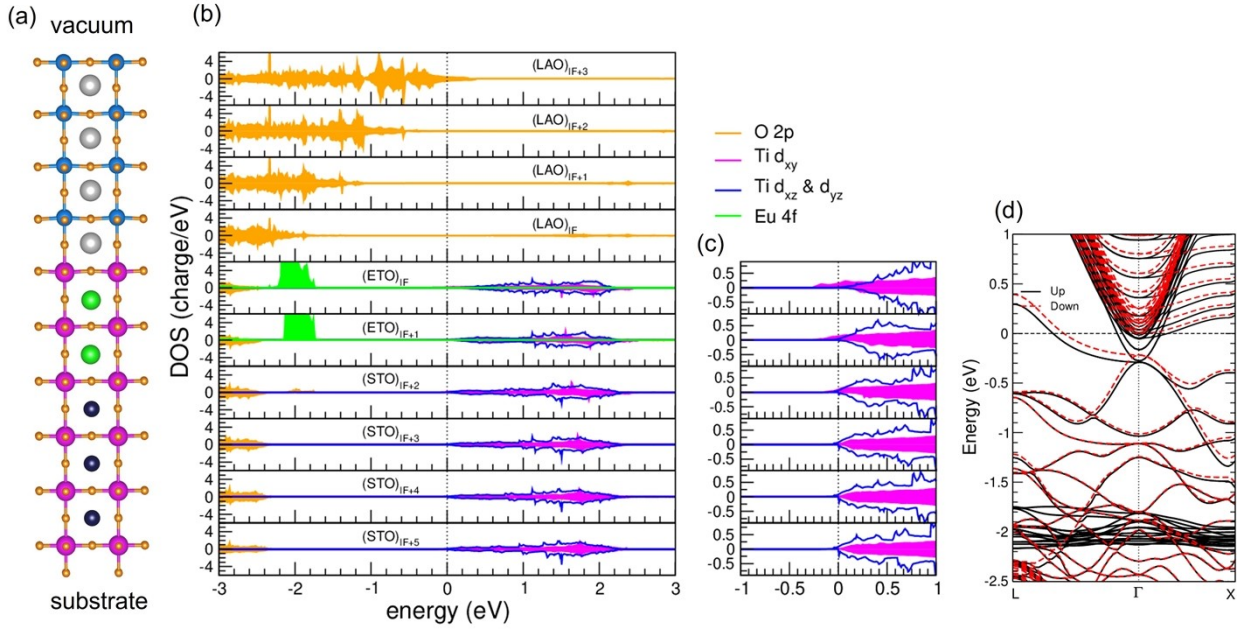

Figure S.1 : ab-initio electronic properties for the STO/ETO/LAO heterostructure with 2 ETO layers at the interface. (a): scheme of the simulation cell structure; atom colors are La (gray), Eu (green), Sr (black), O (orange), Ti (magenta). (b) Orbital-resolved DOS; each panel reports orbitals belonging to the corresponding atomic layer; positive and negative values are for up-spin and down-spin states. Orbital contributions are drawn with different colors specified in the legend; the Fermi energy is fixed to zero, indicated by the vertical dotted line (c) DOS enlargement around the conduction band minimum. (d) band energies for up-spin (black) and down-spin (red dashed) channels

As reported in experiments,[11] the 2DEG is only observed for one or two ETO layers at most, while for 3 or more layers the interface is insulating. This sharp threshold is not motivated by intrinsic properties: considering the virtually identical lattice constant and the very similar dielectric screening of bulk STO and ETO, it is easy to expect that Sr-Eu substitutions do not generate appreciable changes in the charge confinement mechanism. As evidence of this, in Fig. S.1 we display orbital-resolved DOS and band energies for the STO/ETO/LAO heterostructure with 2 ETO layers (2-ETO) at the interface. We can see in Figure S.1b and S.1c that for 2-ETO the 2DEG is still mostly localized within the *3d* t_{2g} orbitals of the two Ti

atoms closer to the interface, with a large predominance of the d_{xy} states. As expected, a significant difference between 1-ETO and 2-ETO is reflected in the magnetization which is much more robust for the latter: large spin splittings of ~ 270 meV and ~ 160 meV now occur for first and second d_{xy} bands from the interface; furthermore, the Eu 4f magnetic moments are so large to induce a visible magnetization even on the O *2p* bands of the LAO overlayer.

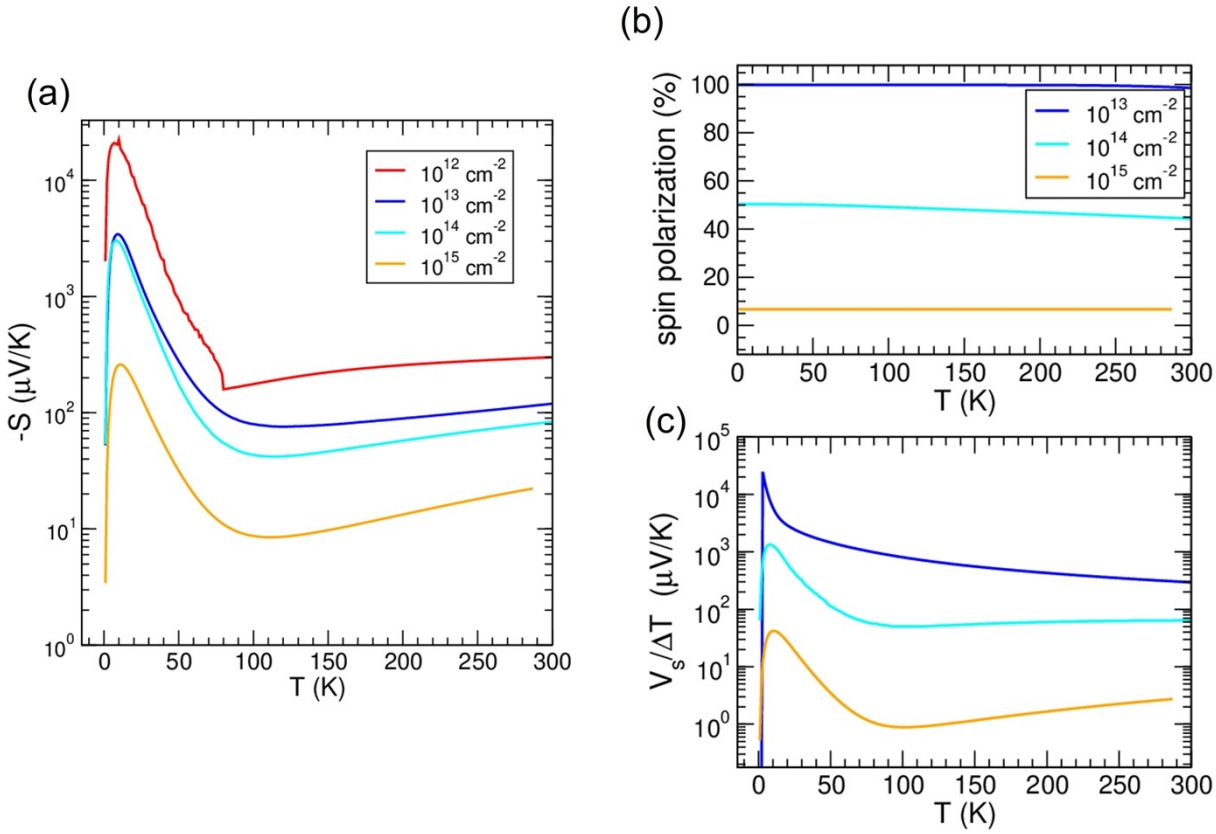

Figure S.2 Thermoelectric properties for the 2-ETO heterostructure. (a) Seebeck coefficient vs temperature, for several carrier densities, indicated in the legend. (b) Spin-polarization fraction vs temperature. (c) spin-voltage to thermal gradient ratio.

In Figure S.2 we report results for Seebeck coefficient (Figure S.2a), spin-polarization fraction (Figure S.2b), and spin voltage to thermal gradient ratio (Figure S.2a) for 2-ETO. Overall, the scenario is very similar to what described for 1-ETO, but some quantitative difference appears: 2-ETO shows slightly larger Seebeck amplitudes and visibly reinforced spin-polarization: for $n = 10^{13}$ cm^{-2} the spin-polarization saturates to the full value in both materials, while for $n = 10^{14}$ cm^{-2} is ~50% for 2-ETO and only about 40% in 1-ETO; this is reflected in the spin voltage, which is similar at $n = 10^{13}$ cm^{-2}, but about an order of

magnitude larger for 2-ETO at $n = 10^{14}$ cm^{-2}. However, for the charge density range where thermal-spin conversion is most effective ($n \sim 10^{13}$ cm^{-2} or smaller) we should expect 1-ETO and 2-ETO to deliver similar performances.

BIBLIOGRAPHY

1) Baylin, M., Transport in Metals: Effect of the Nonequilibrium Phonons, *Phys. Rev.* **112,** 1587–1598 (1958**)**;
2) Baylin, M., Phonon-Drag Part of the Thermoelectric Power in Metals, *Phys. Rev.* **157,** 480 (1967**)**
3) Cantrell, D. G. & Butcher, P. N., A calculation of the phonon-drag contribution to the thermopower of quasi-2D electrons coupled to 3D phonons. I. General theory, *J. Phys. C: Solid State Phys.* **20,** 1985–1992 (1987);
4) Cantrell, D. G. & Butcher, P. N., A calculation of the phonon-drag contribution to the thermopower of quasi-2D electrons coupled to 3D phonons. II. Applications, *J. Phys. C: Solid State Phys.* **20,** 1993–2003 (1987)
5) Smith, M. J. & Butcher, P. N., A calculation of the effect of screening on phonon drag thermopower in a Si MOSFET, *J. Phys.: Condens. Matter* **1,** 1261–1273 (1989);
6) Smith, M. J. & Butcher, P. N., Simple models of phonon-drag in 3D and quasi-2D, *J. Phys.: Condens. Matter* **2,** 2375–2382 (1990)
7) Pallecchi, I.; Telesio, F.; Li, D.; Fête, A.; Gariglio, S.; Triscone, J.-M.; Filippetti, A.; Delugas, P.; Fiorentini, V.; Marré, D. Giant Oscillating Thermopower at Oxide Interfaces. *Nat. Commun.* **2015**, *6* (1), 6678.

8) Pallecchi, I.; Telesio, F.; Marré, D.; Li, D.; Gariglio, S.; Triscone, J.-M.; Filippetti, A. Large Phonon-Drag Enhancement Induced by Narrow Quantum Confinement at the LaAlO 3 / SrTiO 3 Interface. *Phys. Rev. B* **2016**, *93* (19), 195309.

9) Callaway, J., Model for Lattice Thermal Conductivity at Low Temperatures, *Phys. Rev.* **113**, 1046–1051 (1959**)**

10) S. Kamba, V. Goian, M. Orlita, D. Nuzhnyy, J. H. Lee, D. G. Schlom, K. Z. Rushchanskii, M. Lezaic, T. Birol, C. J. Fennie, P. Gemeiner, B. Dkhil, V. Bovtun, M. Kempa, J. Hlinka and J. Petzelt, Magnetodielectric effect and phonon properties of compressively strained EuTiO3 thin films deposited on (001)$(LaAlO_3)_{0.29}$-$(SrAl_{1/2}Ta_{1/2}O_3)_{0.71}$, *Phys. Rev. B*., 2012, **85**, 094435.

11) De Luca, G. M.; Di Capua, R.; Di Gennaro, E.; Granozio, F. M.; Stornaiuolo, D.; Salluzzo, M.; Gadaleta, A.; Pallecchi, I.; Marrè, D.; Piamonteze, C.; Radovic, M.; Ristic, Z.; Rusponi, S. Transport Properties of a Quasi-Two-Dimensional Electron System Formed in LaAlO 3 / EuTiO 3 / SrTiO 3 Heterostructures. Phys. Rev. B 2014, 89 (22), 224413.